A NEW MODEL TO CALCULATE THREE-PHASE RELATIVE PERMEABILITIES: APPLICATION AND VALIDATION FOR A SANDSTONE

J.C. MOULU, O. VIZIKA, F. KALAYDJIAN and J.P. DUQUERROIX

Institut français du pétrole[1]

UN NOUVEAU MODÈLE POUR LE CALCUL
DES PERMÉABILITÉS RELATIVES EN ÉCOULEMENT
TRIPHASIQUE : APPLICATION ET VALIDATION
DANS LE CAS D'UN GRÈS

Les écoulements triphasiques en milieu poreux sont généralement décrits par le modèle de Stone (1970). Ce modèle est basé sur des corrélations empiriques appliquées à des résultats d'écoulements diphasiques. Il n'est valable que dans le cas de mouillabilité franche à l'eau et ne peut pas être utilisé comme outil de prédiction.

L'objectif de la présente étude est de développer un modèle mathématique d'écoulement triphasique en évitant toute corrélation empirique. Dans cet article, les conditions de mouillabilité franche à l'eau et d'étalement sont seules étudiées, mais le modèle pourrait être aisément étendu aux cas de mouillabilité à l'huile et même de mouillabilité mixte.

Le modèle est basé sur une description physique appropriée de la distribution et de l'écoulement des trois phases à l'échelle du pore. Le milieu poreux est décrit comme un assemblage de pores fractals, dont la dimension linéaire et la distribution des rayons sont données par la courbe de pression capillaire obtenue par injection de mercure. Les fluides sont supposés s'écouler ensemble dans le même pore fractal, le gaz dans le centre, l'eau au contact des parois et l'huile entre le gaz et l'eau. Les perméabilités relatives sont évaluées en calculant l'écoulement de chaque fluide par la loi de Poiseuille.

Les résultats du modèle sont comparés aux perméabilités relatives obtenues par le calage d'expériences d'injection de gaz. Ces expériences sont aussi simulées en utilisant le modèle de Stone et des résultats d'expériences diphasiques.

A NEW MODEL TO CALCULATE THREE-PHASE
RELATIVE PERMEABILITIES: APPLICATION AND
VALIDATION FOR A SANDSTONE

Three-phase flow in a porous medium is usually described by the Stone model (1970). This model is based on two-phase data and relies on empirical correlations. It is valid only under strong water wettability and recognized as being a poor predictor.

(1) 1 et 4, avenue de Bois-Préau,
92852 Rueil-Malmaison Cedex - France

The goal of the present study is to develop a mathematical model for three-phase flow avoiding any empirical correlations. In this paper, only strong water-wet and spreading conditions are considered. However the model could be relatively easily extended to oil-wet or even mixed-wet conditions.

The model is based on a physically relevant description of phase distribution and flow mechanisms at the pore scale. The porous medium is described as a set of fractal pores, whose linear fractal dimension and size distributions are derived from a mercury intrusion capillary pressure curve. The fluids are allowed to flow together in the same fractal pore, gas in the center, water near the walls and oil in an intermediate phase. The relative permeabilities are evaluated by calculating the flow of each fluid applying Poiseuille's law.

The model results are compared to relative permeabilities obtained by history matching of gas injection experiments. The same experiments are also simulated using Stone's model and laboratory measured two-phase data.

NUEVO MODELO PARA EL CÁLCULO DE LA PERMEABILIDAD RELATIVA, EN PRESENCIA DE CIRCULACIONES TRIFÁSICAS : APLICACIÓN Y VALIDACIÓN EN EL CASO DE ARENISCAS

Las circulaciones trifásicas en medios porosos se describen generalmente por medio del modelo de Stone (1970). Este modelo se funda en las correlaciones empíricas aplicadas a resultados de circulaciones difásicas y únicamente resulta valedero al tratarse de una humectabilidad franca al agua y por ende, no se puede utilizar como herramienta de predicción.

El objetivo del presente estudio consiste en desarrollar un modelo matemático de circulación trifásica evitando cualquier correlación empírica. En este artículo únicamente se han estudiado las condiciones de humectabilidad franca al agua y de esparcimiento, pero, de cualquier modo, el modelo podría ser fácilmente ampliado a los casos de humectabilidad al aceite e, incluso, de humectabilidad mixta.

El modelo se funda en una descripción física adecuada de la distribución y de la circulación de las tres fases a escala del poro. El medio poroso se describe como un conjunto formado por poros fractales, cuya dimensión lineal y la distribución de los radios son dados por la curva de la presión capilar obtenida por inyección de mercurio. Se supone que los fluidos circulan conjuntamente en el mismo poro fractal, el gas por el centro y el agua en contacto con las paredes y, finalmente, el petróleo entre el gas y el agua. Las permeabilidades relativas se evalúan calculando la circulación de cada fluido por aplicación de la ley de Poiseuille.

Se comparan los resultados del modelo con las permeabilidades relativas obtenidas por el resultado de experiencias de inyección de gas. También se simulan tales experiencias utilizando el modelo de Stone y los resultados de experiencias difásicas.

INTRODUCTION

Many attempts to describe multiphase flow behavior in oil reservoirs have addressed the problem of evaluating the relative permeability of each phase in a saturation range corresponding to the one found in the reservoir. This goal can be attained in two different ways: experiments and modeling.

Experimental determination of three-phase relative permeabilities is not a straightforward task. In fact, no direct method exists to measure relative permeabilities during a displacement, especially when all three phases are mobile [1]. On the other hand, the problem is simplified with experiments where one of the three phases is immobile (at its irreducible saturation) [2].

An easier way to obtain directly relative permeability values is the steady-state method. However the use of these relative permeabilities for the simulation of a displacement is questionable [3].

There have been several attempts to model three-phase relative permeabilities [4] and [5]. Models based on a schematic description of the porous medium as a bundle of cylindrical capillaries have not been validated mainly due to lack of experimental results. Moreover, the assumption that is usually made, that the more wetting fluid occupies the smallest pores and the less wetting the largest ones, does not take into account complex fluid-fluid interactions encountered in three-phase flow.

Currently, three approaches are widely used to treat three-phase flow problems:
– use of steady-state experimental data for displacement simulations;
– use of two-phase data to calculate three-phase parameters by means of a model such as Stone's model [6] and [7];
– use of empirical correlations between relative permeabilities and saturations: the well-known power laws in which the coefficients and exponents are fitting parameters.

The aim of this paper is to evaluate experimentally relative permeability values corresponding to the displacement of oil and water by gas injection in a porous medium and to propose a model to calculate them based on relevant physics but simple enough to be easily implemented in a reservoir simulator. The porous medium is described as a bundle of capillaries with their diameter following a power law. The cross-section of this object is fractal and its linear fractal dimension is

found from the capillary pressure curve. Calculation of the three-phase relative permeabilities is achieved by applying Poiseuille's law in each tube and by using experimentally measured relative permeability end-points. The relative permeability values are compared with those obtained by history matching of gas injection experiments.

Three-phase values estimated using Stone's model are also compared with the experimental and calculated relative permeabilities.

1 CURRENTLY USED MODELS

Two types of physical models are based on a pore picture given by a capillary pressure curve:

– The Corey and Burdine type models [4] and [5]. The authors consider a bundle of cylindrical capillaries. The flow of the three phases can be calculated both in drainage and imbibition conditions. The fluids are distributed in the pores of different sizes depending on their wetting characteristics: for water-wet solid, water occupies the smallest pores, gas the largest ones and oil the intermediate size pores.

By applying Poiseuille's law to the fluid i considered to occupy the pores of radius r_i corresponding to the range S_{ir} (residual saturation) to S_i (saturation in place), the general form for the relative permeabilities is the following:

$$k_{ri} = \int_{S_{ir}}^{S_i} r_i^2 \, dS_i$$

The integration of k_{ri} is made easier if an analytical correlation between r_i and S_i exists. This kind of correlation appears in the log-log plot of the capillary pressure curve (obtained by mercury intrusion) as a function of saturation (Fig. 1) which exhibits two different parts: a linear part with a large slope, for a low wetting phase saturation S_w, and the other part with a small slope, a. Thus a simple correlation between r_i and S_i can be written:

$$r_i = \left(S_i * \right)^a$$

where S_i* is a normalized saturation between the irreducible, S_{ir} and the maximum, $S_{i\,max}$, wetting phase saturation.

– The fractal pore type models [8] and [9]. The slope of the sharp linear part of the capillary pressure curve (Fig. 1) is a function of the linear fractal dimension D_L of the porous medium such as:

$$P_c \propto S_w^{\frac{1}{D_L - 2}}$$

where S_w is the saturation of the wetting phase.

The relative permeability of the oil phase calculated for the case of oil displacement by gas in the presence of irreducible water saturation S_{wi} is given by [10]:

$$k_{ro} = \left(S_o + S_{wi} \right)^{\frac{4 - D_L}{2 - D_L}} - S_{wi}^{\frac{4 - D_L}{2 - D_L}}$$

The model has been successfully tested for the case of gas injection at S_{wi} in water-wet porous media and for oil spreading on water in the presence of gas [2].
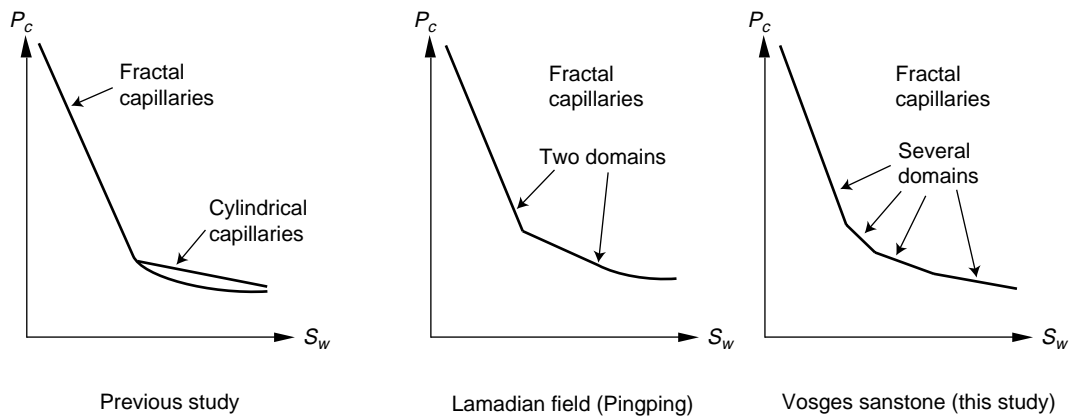

Figure 1

Physical models based on capillary pressure curves.

In the domain of fractal representation of the porous medium, recent papers [11] and [12] present two-phase displacement experiments, capillary pressures obtained by mercury intrusion and Scanning Electron Microscopy (SEM) studies on specific cores (Lamadian reservoir). The authors conclude that three domains are identified by the SEM analysis (Fig. 1), corresponding to three parts on the capillary pressure curve:
  – no fractal with large pores;
  – fractal with large pores;
  – fractal with small pores;

They also relate irreducible water saturation, S_{wi} to the fractal dimension (small pores) and residual oil saturation for water-flooding to the fractal dimension (larger pores).

Since the capillary pressure curve of Vosges sandstone used in the present study shows several domains covering a large saturation range (Fig. 1), it was decided to use a fractal model to calculate the three-phase relative permeabilities with the corresponding fractal dimension for each saturation interval as deduced from the capillary pressure curve.

2 MODELING

The model has to be representative of the real three-phase flow in porous media and to take into account realistic fluid distributions within the porous structure as imposed by the solid-liquid interactions (wettability) and the liquid-liquid interactions (spreading conditions). To this end, the characteristics of a gas injection are first studied. Then, the fractal pore model is described, and the distribution of the fluids in the fractal structure is defined taking into account experimental observations.

3 CHARACTERISTICS OF A GAS INJECTION

The flow of the fluids during gas injection exhibits some particular characteristics:
– At the beginning of the gas injection (as soon as a sufficient gas pressure is applied at the inlet face of the core), the gas phase enters the core and pushes the liquids in place. The liquids are produced, and after a short period of time (usually $\approx 10^3$ s and delayed, $\approx 7 \times 10^3$ s if gas displaces water alone) (Fig. 2) gas appears at the outlet. After gas

breakthrough (BT) and during a long period (up to 10^5 s), the gas saturation, S_g, increases slowly in the core. At the same time oil and water flow at rates, q_o and q_w respectively, such that $dS_g/dt \propto q_o + q_w$. The liquids are replaced by gas which flows through the porous medium along an increasing number of pores independently of the flow of the liquids. After BT, the gas saturation increases slowly from 10% PV up to 40-50% PV and remains roughly uniform along the core (this is verified by the measured saturation profiles) for a long period of time.

– The injection pressure of the gas is relatively high, of the order of 500 mbar. The capillary pressures, obtained by mercury intrusion or with the actual fluids used for the experiments, show that with this injection pressure level, the gas phase can enter a large number of pores (40 to 50% PV) except those occupied by the irreducible water. The lateral expansion of the gas can be considered as cylindrical far from the percolation domain, governed by the probability for the gas to enter only a given range of large pores.
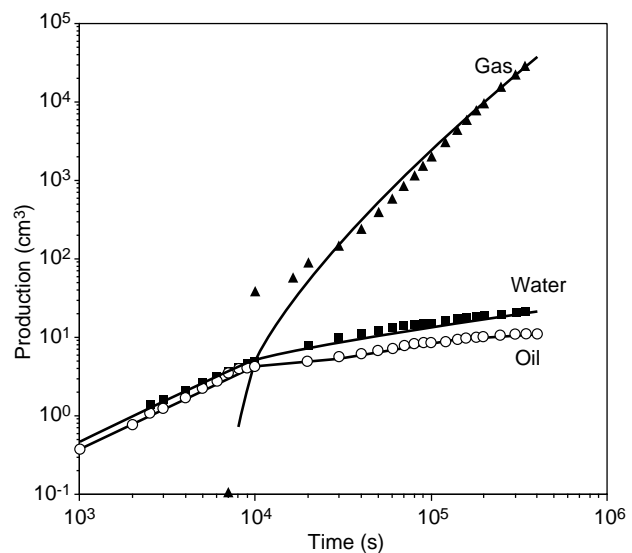

Figure 2

Experimental and simulated production curves (Experiment 2).

These characteristics can be represented if the three fluids flow together in concentric layers within the same pore: the wetting phase (water in this study) flows along the rock walls, the gas phase flows in the center of the pore and oil flows between.

Of course, this picture allows the saturation of each phase to increase or to decrease, pushing the other phases laterally. This study concentrates on the case of an increasing gas saturation, but water imbibitions in oil were also performed.

4 DESCRIPTION OF THE POROUS MEDIUM

The internal surface of a pore is assumed to be a fractal surface. Consequently, a perfectly wetting phase always remains continuous [13]. The isotropic fractal surface is modeled as a bundle of parallel capillary tubes with a fractal cross-section. The cross-section of each tube is constructed by an iterative process, by dividing the half perimeter of a circle into η parts and replacing each part by half a circle (Fig. 3).
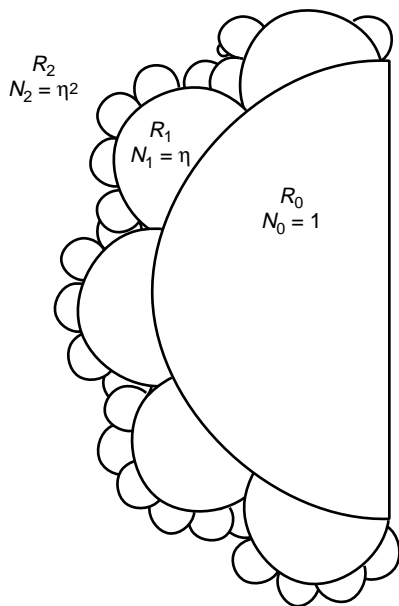

Figure 3

Fractal construction of a pore section.

At each step k of the process, N_k new grooves are created with radius R_k and total cross-section area A_k. These characteristics are given as a function of the initial tube radius R_0 by the following relationships:

$$R_k = \left(\frac{\pi}{2\eta}\right)^k R_0$$

$$N_k = \eta^k$$

$$A_k = \frac{1}{2}\,\pi\,R_0^2\left(\frac{\pi^2}{4\eta}\right)^k$$

The fractal dimension D_L is related to the number of the objects N_k at a given scale l_k, by the relation:

$$N_k \propto l_k^{-D_L}$$

with :

$$l_k = \frac{R_k}{R_0} = \left(\frac{\pi}{2\eta}\right)^k$$

5 SATURATIONS

If only water and oil are involved, and in the case of a water-wet porous medium, oil flows in the bulk of the pore, as is the case for gas in a gas/liquid drainage. In three-phase conditions, water which is considered to be the wetting phase flows along the pore walls, the gas phase flows in the bulk of the pore and oil is sandwiched between the other two. The saturations are calculated as being the relative surface in a cross-section occupied by each fluid.

At equilibrium, all the tubes with size less than or equal to R_k, where R_k is given by Laplace's law: $P_c = 2\gamma\,/R_k$, are occupied by the wetting fluid, and larger tubes by the non-wetting one. Thus, the wetting fluid saturation is given as the surface fraction of the occupied tubes.

The surface fraction of the capillaries occupied by water is calculated from the radius R_k to R_∞. This calculation leads to a series the sum of which is easily calculated to be:

$$S_w = \left(\frac{R_k}{R_0}\right)^{2-D_L}$$

and since:

$$P_c = \frac{2\gamma}{R_k}$$

the correlation between capillary pressure and wetting phase saturation is given by:

$$P_c \propto S_w^{\frac{1}{D_L-2}}$$

where S_w is the wetting phase saturation.

The graphical representation of this correlation in a log-log plot is a straight line starting from the point (S_w, P_c) corresponding to the largest pore with a radius R_0 of the fractal construction.

It can be assumed that (Fig. 4):

– The radius R_0, first invaded when mercury is injected (high wetting phase saturation) corresponds to a value in the range of $1/r = 10^3$.

– Each segment of the capillary pressure curve is a part of a line starting from R_0 (assumed to be the same for all the different segments) and corresponding to the P_c, S_w correlation mentioned above. Each line has a given slope, hence a fractal linear dimension can be deduced. The values of the slope as shown in the figure (from -1.5 to -3.3) lead to values for the linear fractal dimension, D_L, ranging between 1.3 and 1.7.

– Each domain is reached by mercury for saturations corresponding to the place where R_0 is found on each line.
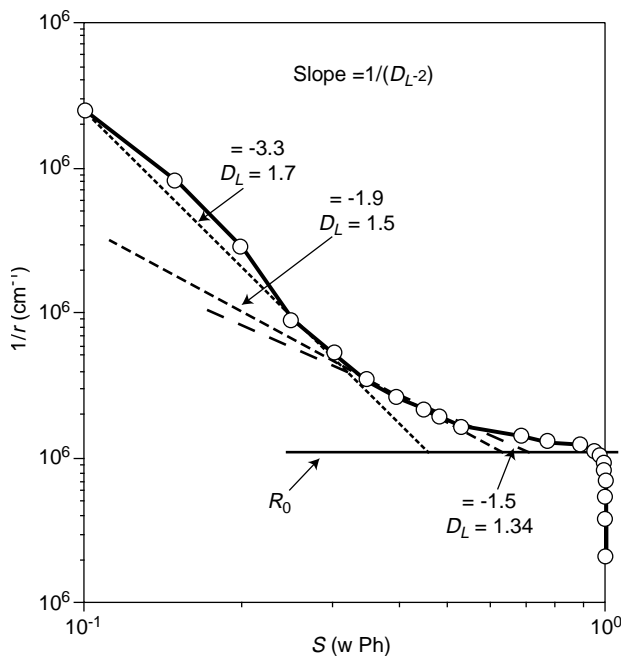

Figure 4

Capillary pressure curve of the Vosges sandstone.

The saturation of two liquids when gas is present in the pore is calculated as explained above for one phase:

$$S_{liq} = \left(\frac{R_k}{R_0} \right)^{2 - D_L}$$

where the two liquids are assumed to occupy the tubes smaller or equal to the radius R_k and the gas the center of each pore.

The oil saturation is the relative surface of the tube cross-section occupied by oil from radius $R_i < R_k$ to R_k.

In order to proceed to the calculation of the relative permeabilities, it is necessary to determine for each phase that part which flows. Therefore, in the following and in a systematic manner, the determination of the relative permeabilities will start with the estimation of the immobile saturations. This will be done for both studied cases, e.g. drainage of water and oil by gas, and water imbibition.

6 RELATIVE PERMEABILITY CALCULATION

6.1 Liquid Relative Permeabilities

To calculate the water and oil relative permeabilities Poiseuille's law is applied in each capillary of the bundle (Fig. 5) occupied by the respective phase.

Taking into account that only the flowing part of the liquids contributes to the hydraulic conductivity, the relative permeabilities for water and oil are calculated to be:

$$k_{rw} = S_w^{\frac{4 - D_L}{2 - D_L}} - S_{wi}^{\frac{4 - D_L}{2 - D_L}} \tag{1}$$

$$k_{ro} = C \left[\left(S_L - S_{org} \right)^{\frac{4 - D_L}{2 - D_L}} - (S_w + S_{orw})^{\frac{4 - D_L}{2 - D_L}} \right] \tag{2}$$

In these expressions, C is a function of S_o, and it is worth mentioning that:

– The irreducible water saturation, S_{wi} is assumed to be immobile.

– S_{orw} is a part of S_o stranded in the water phase and is a function of S_w.

– S_{org} is a part of S_o stranded in the gas phase and is a function of S_g.

– The range of the tubes occupied by flowing oil is calculated as the difference between those occupied
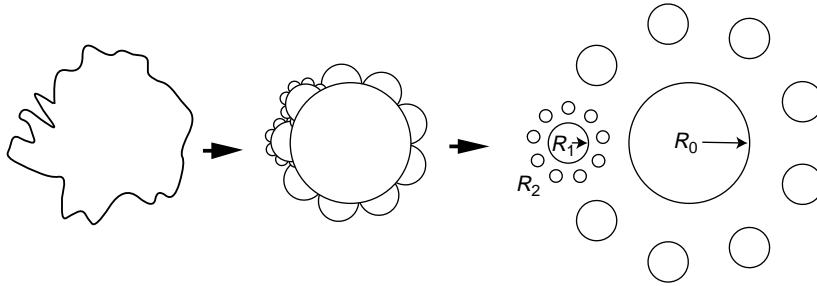
Figure 5

Schematic view of a pore and the tube equivalent used in the calculations.

by the two liquids, with total liquid saturation $S_L = S_o + S_w$, and the ones occupied by water and the immobile oil saturation in water.

6.2 Gas Relative Permeability

Because gas is the non wetting phase, it occupies the porous space starting from the bulk of the pores. As the gas saturation increases, the gas invades the pore laterally, without coming into contact with the solid wall (Fig. 6). It is assumed that gas flows in a single pore with radius given by the following series:
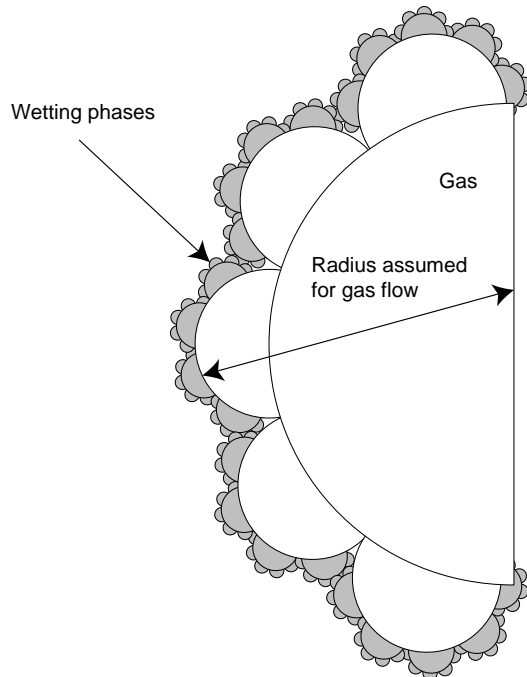
$$R_g = R_0 + R_1 + R_2 + ... R_k \qquad (3)$$

Figure 6

Gas flow in a fractal pore.

With this assumption, the relative permeability to gas is given by:

$$k_{rg} = k_{rg\,max} \left(1 - S_L^{\alpha} \right)^4 \qquad (4)$$

$$\alpha = \frac{1}{2 - D_L}$$

where D_L is the linear fractal dimension of the porous medium and S_L is the total liquid saturation equal to $1 - S_g$.

7 EXPERIMENTAL DETERMINATION OF RELATIVE PERMEABILITIES

7.1 Experiments

Gas injections were performed in porous media containing water and oil under various conditions [1]:
– The porous medium used is a water-wet Vosges sandstone, 40 cm in length, with a relatively low permeability, $K \approx 70 \times 10^{-11}$ cm^2 (70 md) and with a porosity of 0.20.
– The fluids are chosen so as to obtain spreading conditions. The interfacial tensions for the fluid system are: $\gamma_{gw} = 69$ mN/m, $\gamma_{go} = 25$ mN/m and $\gamma_{ow} = 40$ mN/m, and the spreading coefficient is calculated to be:

$$S = \gamma_{gw} - (\gamma_{go} + \gamma_{ow}) = + 4 \text{ mN/m}$$

Before the gas injection different water and oil saturations are obtained:
– either by a water/oil drainage, final oil saturation, S_o and a irreducible water saturation, S_{wi} or imbibition water saturation, S_w and the residual oil saturation, S_{or}, sequence;
– or by a steady-state injection (water and oil injected at a given flow rate ratio). The saturations thus obtained are such that the two liquids are both mobilized by the injected gas.

Gas is injected at a constant pressure (about 500 mbar) and the volume of each effluent is measured with time. The saturation trajectories of the experiments are shown in Figure 7.
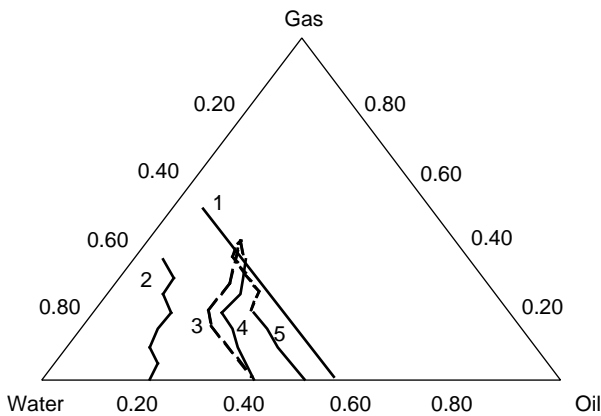

Figure 7

Experimental saturation pathways.

Compared to injection of gas in continuous oil (BT=10^3 s), gas injection in continuous water is characterized by a delayed breakthrough (BT = 7 x 10^3 s).

In all cases, the irreducible water saturation is high (between 0.40 and 0.50 PV). However, this water never gets recovered during the gas injection. On the contrary, the relatively high residual oil saturation, S_{orw}, left behind from a water-flood, is partly swept by gas injection.

7.2 Determination of Relative Permeabilities

A reservoir simulator adapted to laboratory conditions (ΣCORE) is used to simulate the experiments following a procedure already described elsewhere [1]. Relative permeabilities as functions of two saturations, S_g and S_w, and capillary pressure curves (gas-oil and oil-water), are introduced into the simulator according to the following procedure:

- A simplified technique is used to evaluate approximate values of the relative permeabilities in the two-phase and three-phase cases, and to give the curvature of the isoperms.
- With the preliminary values as input, the cumulative oil, water and gas productions are obtained from the simulations.
- Deviations between experimental and calculated production curves indicate the time step, the mean saturation, thus the relative permeability values to be corrected.
- After several iterations, the relative permeability tables give a good fit between experimental and simulated production curves as shown in Figure 2. The relative permeabilities determined this way correspond to the displacements.

Table 1 shows the gas relative permeabilities. In this table, the pathways corresponding to three displacements can be identified. Of course, only relative permeabilities along these saturation pathways are used and then adjusted. In the case of Table 1, the displacements performed are sufficient to fill up

TABLE 1

Gas relative permeabilities

$S_g = 0$	0.01	0.05	0.10	0.15	0.20	0.25	0.30	0.35	0.40	0.45	0.50	0.55	S_w
									.30				0.40
.0 **Displ. 1**	**.002**	**.014**	**.04**	**.08**	**.13**	**.20**	**.27**	**.36** **.28**	**.46**	**.57**	**.69**	**.83**	0.44
		0.007	0.02	0.046	0.081	**.117**	**.205**	0.28	0.39	0.48	0.57		0.50
		0.004	0.011	0.025	**.042**	0.087	0.14	0.22	0.30	0.40			0.55
.0 **Displ. 3**	**.0002**	**.0017**	**.006**	**.0145**	0.032	0.06	**.105**	**.178**	0.25				0.60
		0.0007	0.0025	0.008	0.019	**.037**	0.070	0.11					0.65
		0.0003	0.0012	**.004**	**.01**	0.023	0.045						0.70
		.0001	**.0005**			0.015							0.75
.0 **Displ. 2**	**.0**												0.80

practically the whole table. If this is not the case, the permeability values can be graphically interpolated and a complete table can be established. From these tables, a set of isoperm curves is constructed (Fig. 8) from which the following observations can be made:

– The area of the triangle where the three fluid phases are mobile is very narrow due to the quite high irreducible water saturation.

– It seems difficult to get a consistent view of the water relative permeabilities for the three domains of

saturation that were investigated: the S_{or} case, water imbibition in oil and the three-phase area.

– The gas relative permeability isocurves are practically linear with a slope showing that the gas flows easier with oil (low water saturation) than with water.

– The oil isoperms are curved, as usually observed, showing that for a given oil saturation, the oil relative permeability is decreased by the presence of both water and gas.
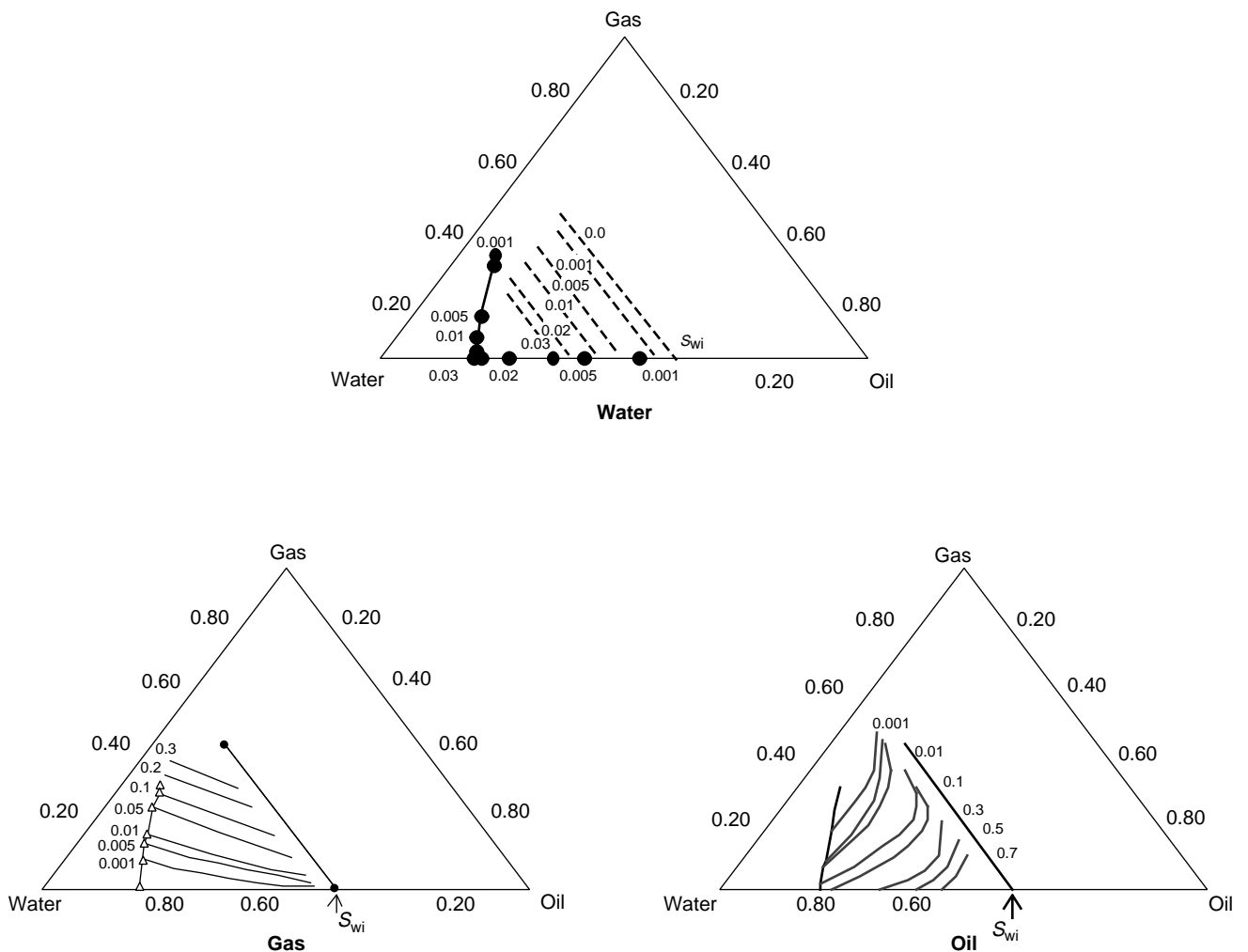

Figure 8

Relative permeability isocurves for the three fluids.

8 DISCUSSION

8.1 Water Relative Permeability

Three sets of curves are displayed in Figure 9. The first two correspond to a gas injection case and depend on whether oil is mobile (G/W+O) or not (G/W+S_{or}). The last one corresponds to an imbibition curve in the case of a water-oil system (W/O).
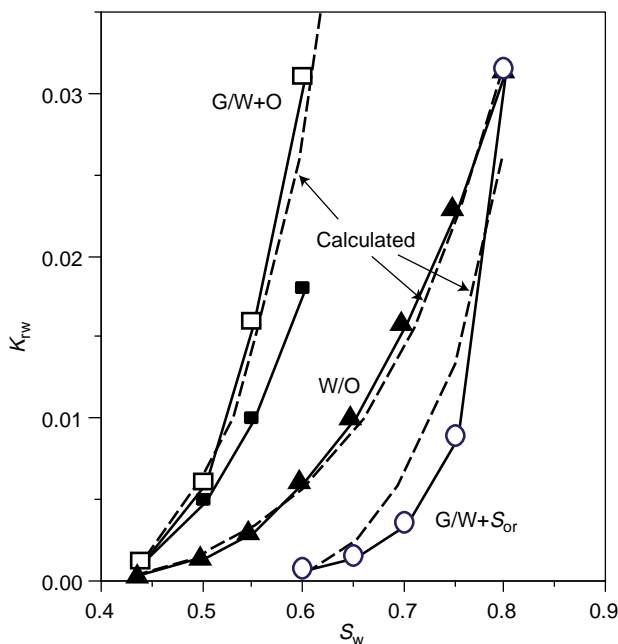
Figure 9

Relative permeability curves for water.

Besides, the ternary diagram (Fig. 7) shows that the irreducible water saturation left in place at the end of the gas injection depends heavily on the initial saturation established before the gas injection:
- If the gas injection starts with a relatively important oil saturation, water is not pushed by gas but by oil if the latter is continuous and the final water saturation is irreducible: S_{wio} left in place by an oil injection.
- On the contrary, a gas injection in the medium containing only oil at the residual saturation leads to a higher final water saturation. In this case, water is pushed directly by gas and, due to the higher interfacial tension value, the sweeping of water by

gas is less efficient than by oil, and the irreducible water saturation finally found, S_{wig} is higher than S_{wio}.

The ternary diagram shows that $S_{wio} = 0.40$ PV and $S_{wig} = 0.57$ PV. The calculation of the radius of a capillary containing water and invaded at a mean pressure of about 250 mbar gives 5.5 µm for a gas injection and 3.2 µm for an oil injection. These values reported on Figure 4 give corresponding water saturations of 50 and 36% PV, in close agreement with the values found experimentally.

The relative permeability curves for a gas injection, when initial water saturation is S_{orw}, show that this extra water saturation of 17% PV is not added to S_{wio} as an irreducible water saturation in the smallest grooves, but is an immobile part of the water phase in larger grooves. This gives:

$$k_{rw} = (S_w - 0.17)^{\beta} - S_{wio}^{\beta} \qquad (5)$$

The calculation of water relative permeabilities with Equations (1) and (5) gives a good fit of the k_{rw} curves as shown in Figure 9,

with: $\qquad \beta = \dfrac{4 - D_L}{2 - D_L} \ = 7.7 \ (D_L = 1.7)$

It is likely that the immobile water, S_{wim}, found in the S_{or} case is put in place during the water imbibition, and reaches 17% PV at the end of the imbibition. A linear correlation gives the value of the extra immobile water saturation as a function of the total water saturation. The mobile water saturation, put in Equation (1) gives a calculated curve very similar to the experimental one (Fig. 9).

8.2 Gas Relative Permeability

The gas relative permeability table (k_{rg} as a function of S_g and S_w) obtained by matching the experimental data is plotted in Figure 10.

The following assumptions are verified first:
- The capillary pressure curve gives the fractal dimension of the porous medium as a function of the wetting phase saturation.
- The flow of gas takes place in a pathway having a radius given by Equation (3).

The experiment the most similar to a mercury intrusion would be a gas injection in the porous

medium containing only water. In this case, the flow of gas would satisfy the two assumptions. This kind of experiment was not performed during this study, but it can be supposed that the corresponding relative permeability values are given by extrapolation of the k_{rg} curves up to S_g such as $S_o = 0$ (only gas and water in place) as shown in Figure 10.
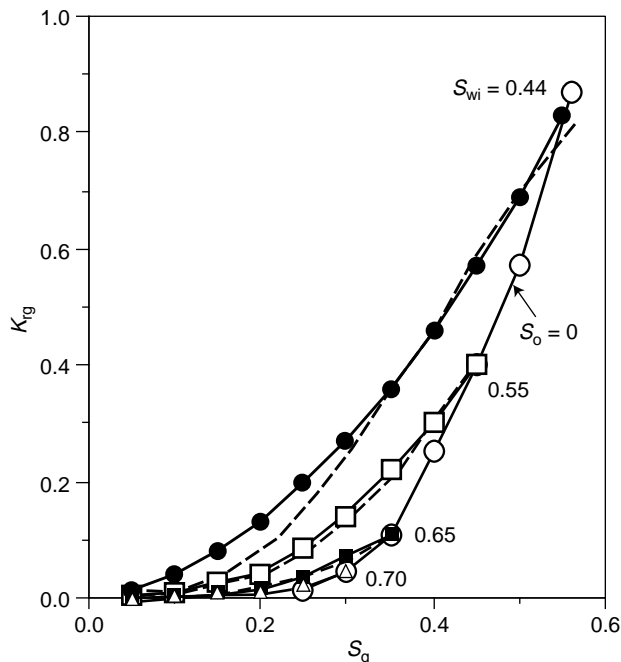

Figure 10

Relative permeability curves for gas.

The slope of the P_c curve gives the value of D_L for various S_w (wetting phase or water) (Fig. 4). The calculation of k_{rg} with Equation (4) gives a good approximation of the k_{rg} values for the points $S_o = 0$ thus verifying the second assumption. The calculation of k_{rg} in the general case when oil is also present can be performed, remembering that to each curve with $S_w =$ const. corresponds one value for D_L.

A good fit is obtained except for the lowest gas saturations, roughly before breakthrough, where the fractal model cannot be applied. $k_{rg\ max}$ is the value of the gas relative permeability for $S_L = 0$. This value is found by writing the condition $k_{rg} = 1$ for $S_w = 0.4$ PV, as suggested by the results of the experiment simulations, and it turns out that $k_{rg\ max} = 1.12$.

8.3 Oil Relative Permeability

The results of the simulations constitute a set of oil relative permeability curves as a function of S_g (Fig. 11) for various values of the water saturation.

The pathways of the displacements in the ternary diagram (Fig. 7) show that, starting with a continuous oil phase, the final oil saturation left in place by the gas, S_{or}, has mainly two different values:

- $S_{org} = 0.05$ and $S_{orw} = 0$ in case of irreducible water saturation S_{wi} when oil is initially continuous within the core.
- $0.10 < S_{orw} < 0.15$ in all other cases, when at water saturations higher than S_{wi}, part of the oil is completely trapped and thus not accessible to gas.
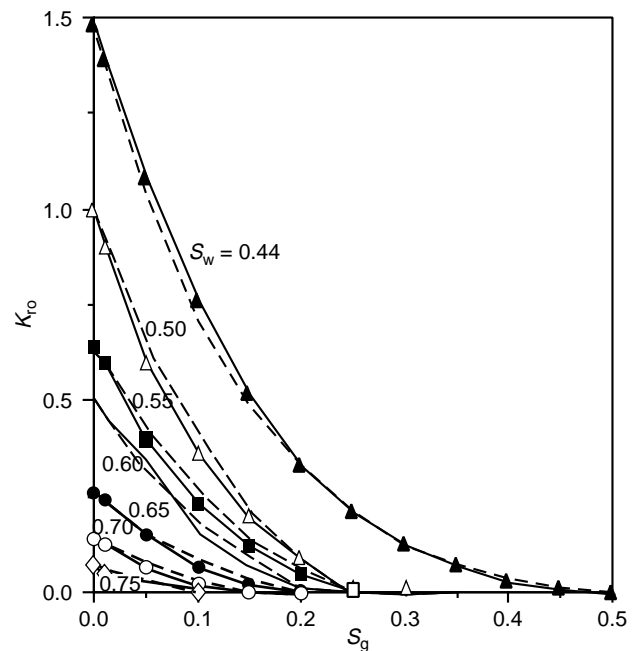

Figure 11

Relative permeability curves for oil.

The expression for k_{ro} (Equation (2)) applied here shows that oil relative permeability is very sensitive to both the fractal dimension, D_L, and the immobile oil saturation for a given water saturation, S_{or}, however a good fit is obtained as shown in Figure 11.

8.4 Comparison with Stone's Model

Based on the analytical expressions for the three-phase relative permeabilities described above, a program was developed to provide the reservoir simulator with the required input.

Two-phase and three-phase relative permeabilities depending on two saturations are derived from the analytical model which corresponds to the fractal description.

Comparisons were done between the analytical model and Stone I formulation. For Stone I, a linear evolution of the minimum oil saturation as a function of gas saturation is considered. Due to the relatively high pressure drop applied, capillary pressure has no influence on the simulation results. Among the simulations carried out, two representative cases are presented here. The experiments were simulated using ATHOS R, a multipurpose, compositional, three-phase and 3-D reservoir simulator. Both classical relative permeabilities and three-phase relative permeability tables, depending on two saturations can be introduced in the simulator.

The two representative cases investigated are as follows:

- Experiment 1, conducted at the irreducible water saturation, in which case, only gas and oil are mobile;
- Experiment 5 started at intermediate oil saturation.

The main features of these experiments are reported in Table 2. Thirty cells along the core were considered for the simulations.

TABLE 2

Simulations with Stone's model

Experiment	ϕ	K (μm^2)	S_{wi}	S_{org}	Recovery OOIP (%)
1	0.1726	56 10^{-3}	0.44	0.05	81
5	0.1726	27.6 10^{-3}	0.40	0.15	67

In Experiment 1, there was no water production, and, in this situation, the two-phase Stone's model does not differ from the analytical solution.

In Experiment 5, the initial oil saturation corresponds to an intermediate situation. Physically, gas pushes oil which in turn pushes water and again this does not correspond to Stone's assumptions where water and gas flow independently in the core. Stone I predictions are far from the experimental data (Figs. 12 and 13).

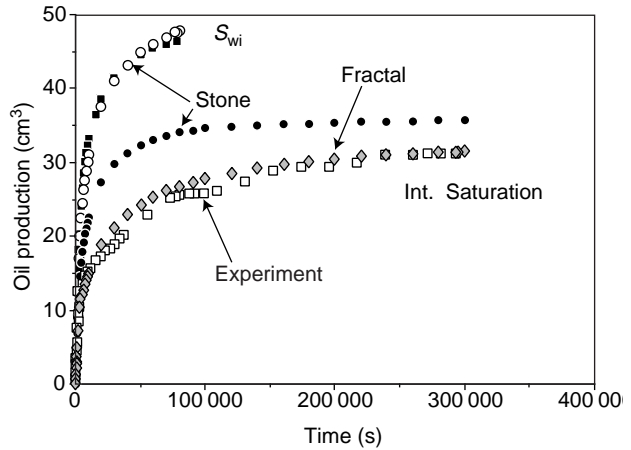We conclude that, under real three-phase conditions, Stone's model cannot represent the experiments.

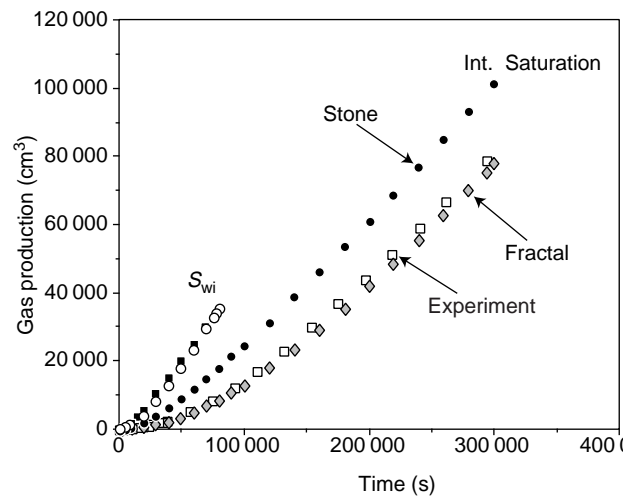Figure 12

Comparison of oil productions.

Figure 13

Comparison of gas productions (experiments and calculation).

CONCLUSIONS

A model for the pore structure of a porous medium based on the mathematics of fractal geometry was used to derive analytical expressions for three-phase water, oil and gas relative permeabilities.

In the new model, relative permeabilities are given as power law functions of the saturations. The exponents

depend on the fractal dimension of the porous medium, D_L, which can be derived from the capillary pressure curve for a given wetting phase saturation. In the case of the porous medium used in this study D_L ranges between 1.3 and 1.7.

The new model was successfully tested against experimental curves derived by history matching of various gas injection processes in a porous medium containing oil and water.

The main features characterizing this new model are:

– Water relative permeability is a function of the water saturation alone. The fractal dimension used for the calculation ($D_L = 1.7$) indicates that water flows in the smallest grooves in direct contact with the pore walls.

– Oil relative permeability is a function of the water and gas saturations. The residual oil saturation is also an important parameter affecting the shape of the curves.

– Gas relative permeability is a function of water and gas saturation, contrary to the classical Stone model.

The results of the fractal model were compared with Stone's model, and it has been verified that this model gives good results only in the cases where only two fluids are mobile.

The fractal model should be extended and tested for the case of a WAG process that constitutes a classic, though complex, three-phase displacement.

NOMENCLATURE

a	exponent in Corey and Burdine model
A_k	area of the grooves of step k
BT	gas breakthrough
D_L	fractal dimension
K	permeability (m^2)
k_r	relative permeability
k_{ro}	oil relative permeability
k_{rg}	gas relative permeability
k_{rw}	water relative permeability
k_{ri}	relative permeability of fluid i
k	permeability (m^2)
$k_{rg\,max}$	maximum gas relative permeability
l_k	scale at the step k
N_k	number of objects of step k
P_c	capillary pressure (N/m^2)

PV	pore volume (m^3)
q_o	oil flow rate
q_g	gas flow rate
q_w	water flow rate
R_0	initial capillary tube radius (m)
R_i	other capillary radius (m)
i	1 ,2, ... k step of the fractal construction
R_g	fractal radius of gas flow
S	saturation
S	spreading coefficient
S_g	gas saturation
S_i	saturation of fluid i
$S_{i\,max}$	maximum saturation of fluid i
S_i^*	normalized saturation of fluid i
S_{ir}	irreducible saturation of fluid i
S_L	$S_o + S_w$
S_o	oil saturation
S_o^*	mobile oil saturation
S_{orw}	residual oil saturation in the water phase
S_{org}	residual oil saturation in the gas phase
S_w	water saturation
S_{wi}	irreducible water saturation
S_{wio}	irreducible water saturation to an oil injection
α	$1/(2 - D_L)$
β	$(4 - D_L)/(2 - D_L)$ exponent in Equation (5)
γ_{ij}	interfacial tension (mN.m^{-1})
ij	g_w, g_o, o_w
η	number of new tubes created at each step.

REFERENCES

1 Moulu J.C., Kalaydjian F. and Martin J.M. (1995) Performance and Numerical Interpretation of Gas Drainage Core Tests under Secondary and Tertiary Conditions, *Paper SCA 9508, presented at the SCA Symposium, San Francisco*, Sept. 12-14,.

2 Kalaydjian F. J.M., Moulu J.C., Vizika O. and Munkerud P.K. Three-phase flow in water-wet porous media: determination of gas/oil relative permeabilities under various spreading conditions, *Paper SPE 26671, presented at the 1993 SPE Annual Technical Conference and Exhibition, Houston, Texas* (Oct. 3-6).

3 Kalaydjian F.J.M., Vizika O., Moulu J.C. and Munkerud P.K. (1995) Role of Wettability and Spreading on Gas Injection Processes under Secondary Conditions, *de Haan H.J. (ed.)*, New Developments in Improved Oil Recovery, *Geological Society Special Publication* 84, 63-71.

4 Burdine N.T. (1953) Relative permeability calculations from pore size distribution data *Trans AIME*, 198, 71-78.

5 Corey A.T. (1954) The interrelation between gas and oil relative permeabilities, *Prod. Monthly,* 19, 38.

6 Stone H.L.(1970) Probability Model for Estimating Three-Phase Relative Permeability, *J. Pet. Tech.*, 22, 214-218.

7 Stone H.L. (1973) Estimation of Three-Phase Relative Permeability and Residual Oil Data, *J. Can. Pet. Tech.*, 12, 4 53-61.

8 De Gennes P.G. (1985) Partial filling of a fractal structure by a wetting fluid Physics of Disordered Materials 227-241, *New York: Plenum Pub. Corp*.

9 Lenormand R. (1990) Gravity-assisted inert gas injection: micromodel experiments and model based on fractal roughness, The European Oil and Gas Conference, *Altavilla Milica, Palermo, Sicily*, October 9-12.

10 Vizika O. (1993) Effect of the Spreading Coefficient on the Efficiency of Oil Recovery with Gravity Drainage, Symposium on Enhanced Oil Recovery, 205th National *Meeting of ACS, Denver CO*, March 28.

11 Pingping S. and Kevin L. A new method for determining the fractal dimensions of pore structure and its application. Paper OSEA-94092 presented at the 1994 *Offshore East Asia Conference, Singapore,* Dec. 6-9.

12 Pingping S., Kevin L. and Fenshu J. Quantitative description for the heterogeneity of pore structure by using mercury capillary pressure curves. Paper SPE 29996 presented at the 1995 International Meeting of Petroleum Engineering, *Beijing, PR China,* Nov. 14-17.

13 Vizika O. and Lenormand R. (1991) Flow by Film of the Wetting Phase in a Porous Medium and its Role on the Gravity Drainage Process, *presented at the IEA 12th International Workshop and Symposium, Bath UK*, October 28-30.